

## Article

# Morphological and Molecular Analysis Describing Two New Species of *Myxobolus* (Cnidaria, Myxosporea) in *Mugil curema* (Mugilidae) from Brazil <sup>†</sup>

Diego Henrique Mirandola Dias Vieira <sup>1,\*</sup>, Melissa Miyuki Osaki-Pereira <sup>1</sup>, Vanessa Doro Abdallah <sup>2</sup>, Sarah Letícia Paiva Oliveira <sup>2</sup>, Aline Gabriely Torres Duarte <sup>2</sup>, Reinaldo José da Silva <sup>1</sup> and Rodney Kozlowiski de Azevedo <sup>3</sup>

- <sup>1</sup> Division of Parasitology, Institute of Biosciences, São Paulo State University (Unesp), Botucatu 18618-689, São Paulo, Brazil; melissamopereira@gmail.com (M.M.O.-P.); reinaldo.silva@unesp.br (R.J.d.S.)
- <sup>2</sup> Parasitology and Pathology Sector, Institute of Biological and Health Sciences, Federal University of Alagoas, Maceió 57072-970, Alagoas, Brazil; vanessaabadallah@gmail.com (V.D.A.); sarah.oliveira@icbs.ufal.br (S.L.P.O.); aline.duarte@icbs.ufal.br (A.G.T.D.)
- <sup>3</sup> Postgraduate Program in Environmental Systems Analysis, CESMAC University Center, Maceió 57051-160, Alagoas, Brazil; azevedork@gmail.com
- \* Correspondence: diegovieira.50@gmail.com
- <sup>†</sup> urn:lsid:zoobank.org:pub: DF7A41CE-371F-436A-91DD-5A488DF2586E,  
urn:lsid:zoobank.org:act:F8374B6D-4C92-40AB-A814-424E32558172,  
urn:lsid:zoobank.org:act:CA99B87B-C8CF-4D71-AEFA-52752360A55B.



**Citation:** Vieira, D.H.M.D.; Osaki-Pereira, M.M.; Abdallah, V.D.; Oliveira, S.L.P.; Duarte, A.G.T.; da Silva, R.J.; de Azevedo, R.K. Morphological and Molecular Analysis Describing Two New Species of *Myxobolus* (Cnidaria, Myxosporea) in *Mugil curema* (Mugilidae) from Brazil. *Taxonomy* **2024**, *4*, 548–560. <https://doi.org/10.3390/taxonomy4030026>

Academic Editor: Mathias Harzhauser

Received: 14 April 2024  
Revised: 10 July 2024  
Accepted: 15 July 2024  
Published: 30 July 2024



**Copyright:** © 2024 by the authors. Licensee MDPI, Basel, Switzerland. This article is an open access article distributed under the terms and conditions of the Creative Commons Attribution (CC BY) license (<https://creativecommons.org/licenses/by/4.0/>).

**Abstract:** We present descriptions of two newly discovered species of *Myxobolus* (Myxobolidae) that infect *Mugil curema*: *Myxobolus mundauensis* n. sp. found in gills and *Myxobolus patriciae* n. sp. found in intestines. These descriptions are based on the morphology of myxospores, histological analysis, and sequencing of the small subunit ribosomal DNA (ssrDNA). The myxospores of both species differ in the width and length of their spore bodies, and their ssrDNA sequences showed a 10.6% difference. These findings support the identification of these parasites as distinct and previously unknown species. Phylogenetic analysis revealed a subclade consisting of species that parasitize Mugiliformes, with *Myxobolus mundauensis* n. sp. being closely related to *Myxobolus maceioensis*, and *Myxobolus patriciae* n. sp. being closely related to *Myxobolus curemae*. Our analysis aligns with previous research suggesting a strong correlation between host orders and phylogenetic patterns within the Myxobolidae family.

**Keywords:** *Myxobolus patriciae* n. sp.; *Myxobolus mundauensis* n. sp.; phylogeny; taxonomy; Mundaú Lagoon; molecular analysis

## 1. Introduction

*Mugil curema* Valenciennes, 1836 belongs to the family Mugilidae Jarocki, 1822, and these fish are known as “white mullets”. *Mugil curema* inhabits a range of environments, predominantly coastal and estuarine [1–5], that are distributed from the United States to southern Brazil [1,6,7]. In Brazil, they are predominantly found in the northeast region [6,8]. These fish are used commercially through fishing and aquaculture and are an important food source [4,9,10].

Myxozoans, increasingly recognized as widespread and diverse endoparasitic cnidarians, constitute vital components of ecosystems [11]. While fish primarily serve as hosts for myxozoans, some species also parasitize other classes of animals [12]. *Myxobolus* Bütschli, 1882, the largest genus within the family Myxosporea Bütschli, 1881, encompasses over 1000 identified species [13]. These parasites are known to infest a multitude of organs across approximately sixteen fish orders in the Americas [12–14].

There are several *Myxobolus* spp. described that parasitize different organs of mugilids [15–20]. Regarding *M. curema*, two *Myxobolus* spp. that parasitize the gills were recently described: *Myxobolus curemae* Vieira, Agostinho, Negrelli, Silva, Azevedo, and Abdallah, 2022, which parasitizes hosts from southeastern Brazil, and *Myxobolus maceioensis* Vieira, Agostinho, Negrelli, Silva, Azevedo, and Abdallah, 2022, which parasitizes hosts from northeastern Brazil. *Myxobolus hani* Faye, Kpatcha, Diebakate, Fall, and Toguebaye, 1999 parasitizes the branchial spines of the gill arch of *M. curema*, which was collected off Senegal [21]. In addition to these species, there is a report that *Myxobolus* sp. parasitizes the heart of *M. curema*, which was collected from the Atlantic Ocean off Senegal [22].

During a survey of myxozoan parasites isolated from *M. curema*, plasmodia-containing myxospores consistent with *Myxobolus* were observed in gills and intestines. Herein, we use morphology, histology, and phylogenetics to describe the new species of *Myxobolus*.

## 2. Materials and Methods

### 2.1. Host Sampling and Morphological Analysis

*Mugil curema* were obtained fresh from fishermen who commercialize this type of fish at Mundaú Lagoon located in Maceió (n = 42), Alagoas, Brazil (9°37'36.5" S 35°47'06.3" W). Host specimens were examined, with both internal and external organs evaluated to locate plasmodia-containing myxospores, using a Leica S6 D stereomicroscope (Leica Microsystems, Wetzlar, Germany). Plasmodia were extracted, prepared between a slide and coverslip, and analyzed using light microscopy. Mature myxospores belonging to the genus *Myxobolus* were identified in the gills and intestines of the infected hosts. Tissue samples hosting plasmodia were collected for morphological and molecular analysis.

Measurements of 30 myxospores from each myxozoan species from one fish specimen were made using a differential interference contrast microscope (DIC) at 1000× magnification. Digital images of the spores were obtained, and their measurements were taken with the assistance of Leica LAS V3.8 software (Leica Application Suite, V3; Leica Microsystems, Wetzlar, Germany). Myxospores were measured according to the methods outlined by Lom and Arthur (1989) [23], with a focus on spore size, polar capsule size, and the number of turns of the polar filament. All measurements are presented in micrometers (µm) and are expressed as a range, along with the corresponding means ± standard deviations. The prevalence of infection was calculated according to the methodology described by Bush et al. (1997) [24].

### 2.2. Molecular and Phylogenetic Analysis

Plasmodia-containing samples of the host's gills and intestine were stored in absolute ethanol for DNA extraction. The procedures followed the animal tissue protocols of the DNeasy® Blood & Tissue Kit (Qiagen, Valencia, CA, USA). Access to the genetic data was authorized by the Brazilian Ministry of Environment (Sisgen A425DD8). The primers used are shown in Table 1. The polymerase chain reaction (PCR) conditions and parameters used were the same as those used by Vieira et al. (2022) [25]. The polymerase chain reactions (PCRs) were carried out at a final volume of 25 µL using PCR Ready-to-Go beads (Pure Taq™ Ready-to-Go™ beads, GE Healthcare, Chicago, IL, USA) and contained 20–40 ng of extracted DNA, 10 pmol of each primer, and 20 µL of distilled water. Amplifications were performed on a Bio-Rad MJ Mini Gradient Thermal Cycler (Bio-Rad Laboratories, PA, USA), with an initial denaturation at 95 °C for 3 min, followed by 35 cycles of 95 °C for 1 min, annealing at 55 °C for 45 s, and 72 °C for 2 min, and a final extension at 72 °C for 7 min. The PCR products were analyzed via electrophoresis, with GelRed staining of a 1% agarose gel in a Tris–acetate–EDTA buffer (Tris 40 mM, acetic acid 20 mM, EDTA 1 mM) followed by visualization under UV light. Amplicon sizes were estimated by comparing each one with the 1 kb Plus DNA Ladder (Invitrogen, Thermo Fisher Scientific, Waltham, MA, USA). The PCR reaction products were purified with magnetic beads from the Ampure XP kit (Beckman Coulter, Brea, CA, USA) following the manufacturer's protocol and sequenced using the same PCR amplification primers. DNA amplification was conducted using the Bio-Rad Mycycler thermocycler (Bio-Rad Laboratories

Ltd., Gladesville, Australia). The resulting PCR product was subjected to electrophoresis on a 1% agarose gel in TAE buffer, alongside a 1 kb DNA ladder (Invitrogen, Thermo Fisher Scientific, Waltham, MA, USA) and visualized under UV light. Following this, the PCR product was purified and sequenced utilizing the BigDye<sup>®</sup> Terminator v3.1 Cycle Sequencing Kit (Applied Biosystems, Waltham, MA, USA), employing an ABI3730xl automatic DNA analyzer (Applied Biosystems, Waltham, MA, USA), and precipitated through an ethanol/EDTA/sodium acetate reaction as per the manufacturer's instructions.

**Table 1.** Primers used for the amplification and sequencing of the *ssrDNA* of the new *Myxobolus* spp.

Primer	Sequence 5'-3'	Paired with	Reference
Erib1	ACCTGGTTGATCCTGCCAG	Act1r	[26]
Myxgen4F	GTGCCTTGAATAAATCAGAG	Erib10	[27]
Act1r	AATTCACCTCTCGCTGCCA	Erib1	[28]
Erib10	CTTCCGCAGGTTACCTACGG	Myxgen4F	[26]
MB5	GGTGATGATTAACAGGAGCGGT	MX3	[29]
MX3	CCAGGACATCTTAGGGCATCACAGA	MB5	[30]

Contiguous sequences were assembled and edited in Sequencher v. 5.2.4 (Gene Codes, Ann Arbor, MI, USA) and subjected to Basic Local Alignment Search Tool (BLAST) analysis (<http://blast.ncbi.nlm.nih.gov> accessed on 10 December 2023) to confirm their identity. The consensus sequences of the *Myxobolus* *ssrDNA* gene were aligned using the Geneious 7.1.3 software [31] with ClustalW [32] to compare with other partial sequences of related species of myxozoans available on GenBank. The outgroup used was *Myxidium ceccarellii* (KJ499821).

Phylogenetic analyses were conducted using Bayesian inference (BI) and maximum-likelihood (ML) methods. Bayesian inference was carried out using MrBayes 3.1.2 [33], employing a GTR+I+G evolutionary model. Markov Chain Monte Carlo analysis was executed for 10 million generations, with log-likelihood scores plotted. The burn-in, comprising the initial 25% of generations, was discarded, and the consensus tree (majority rules) was generated from the remaining topologies. Nodes with posterior probabilities exceeding 90% were considered strongly supported. ML analyses were performed using RAxML v8 [34] on the CIPRES online platform [35], with 1000 bootstrap replications. Nodes with bootstrap values exceeding 70% were deemed well-supported. The tree generated after the BI and ML was analyzed in Figtree 1.4.2 [36] and edited in CorelDraw<sup>®</sup> (CorelDraw Graphics Suite, version x8, Corel Corporation, Ottawa, ON, Canada).

### 3. Results

From 42 specimens of *M. curema* from Mundaú lagoon, six (14.3%) had plasmodia of an unknown species of *Myxobolus* in the gill lamellae (Figure 1A) and five (11.9%) had plasmodia of an unknown species of *Myxobolus* in the intestine (Figure 1B,C). Only one host specimen was parasitized in the gills and intestine simultaneously. Below is the description of the two novel species, based on morphological data, *ssrDNA* sequencing, and information regarding their phylogenetic relationship.

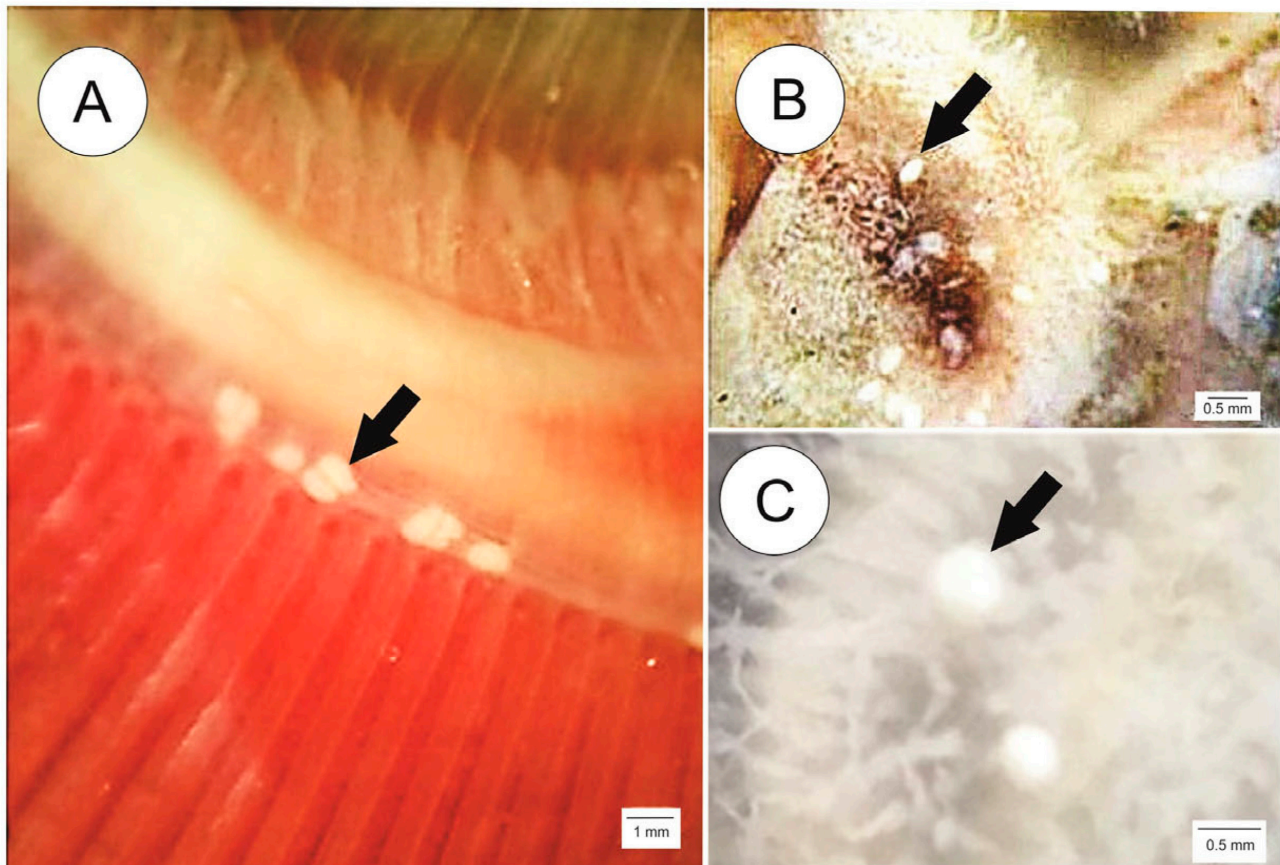


**Figure 1.** (A–C) Myxozoans parasitizing *Mugil curema* from the Mundaú Lagoon. (A): Plasmodia of *Myxobolus mundauensis* n. sp. in the base of the lamella of the gills (black arrow). (B): Plasmodia (black arrow) of *Myxobolus patriciae* n. sp. in the lamina propria of intestines. (C): Details of the plasmodia of *Myxobolus patriciae* n. sp. (black arrow).

### 3.1. Species Description

#### 3.1.1. Taxonomic Summary

Phylum Cnidaria Verrill, 1865

Subphylum Endocnidozoa Schuchert, 1996

Class Myxozoa Grassé, 1970

Subclass Myxosporea Bütschli, 1881

Order Bivalvulida Shulman, 1959

Family Myxobolidae Thélohan, 1892

Genus *Myxobolus* Bütschli, 1882

*Myxobolus mundauensis* n. sp. (Figures 2A–D and 3A)

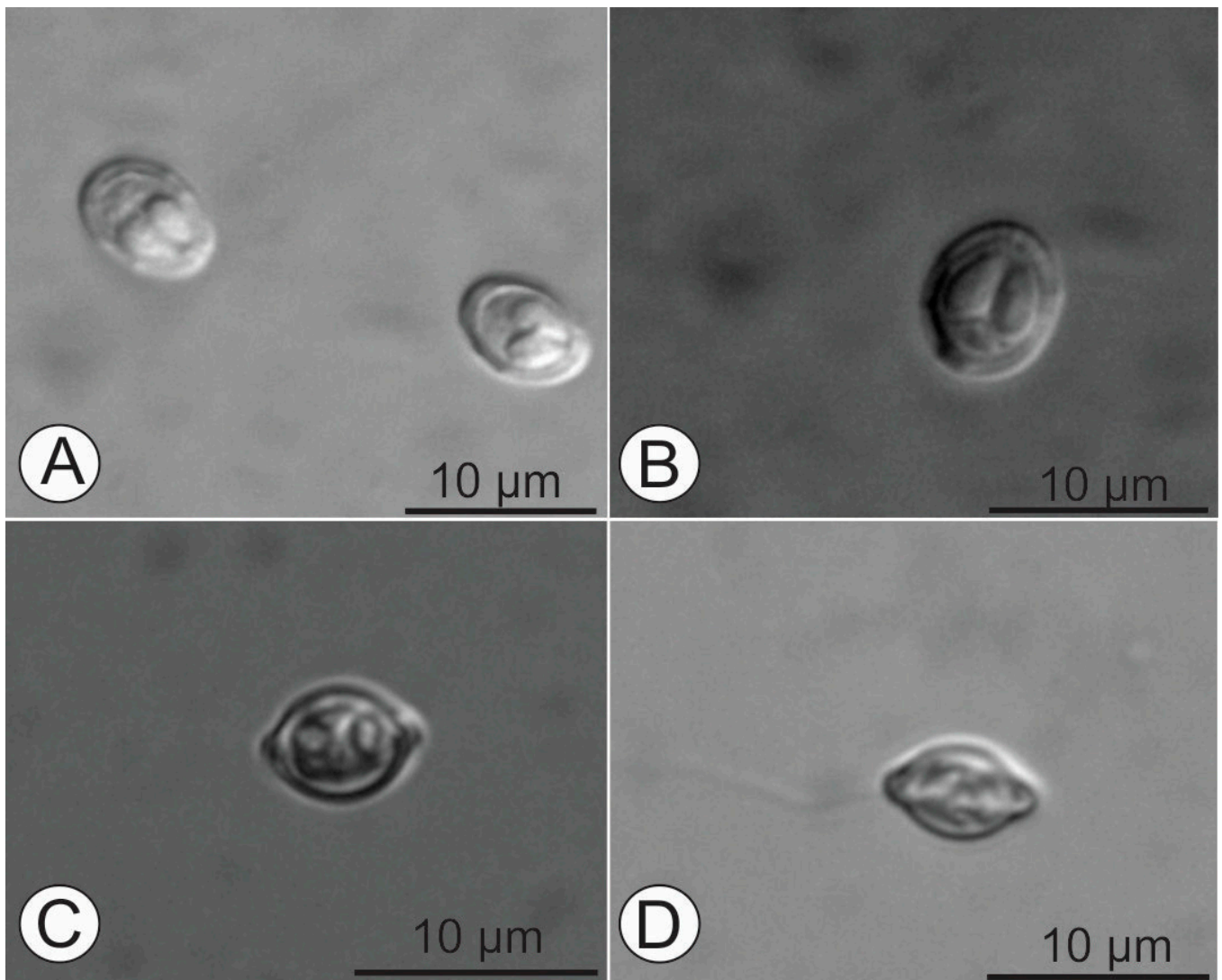


**Figure 2.** (A–D) Mature myxospores of *Myxobolus mundauensis* n. sp. (INPA–CND 000105) found parasitizing the gills of *Mugil curema*; (A,B): frontal view; (C): apical view; (D): side view.

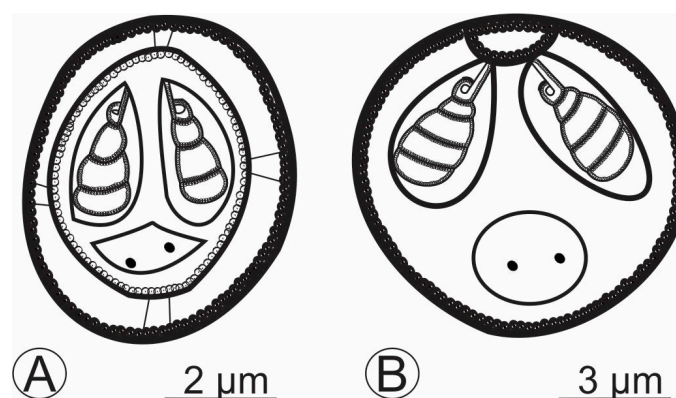


**Figure 3.** (A,B) Schematic drawing of the new species of *Myxobolus* described in this study. (A): *Myxobolus mundauensis* n. sp. (B): *Myxobolus patriciae* n. sp.

Type-host: *Mugil curema* Valenciennes, 1836 (Mugiliformes, Mugilidae).  
Prevalence: 6 of 42 (14.3%) fish.

Intensity: on average one plasmodium per parasitized host.

Type-locality: Mundaú lagoon, municipality of Maceió, Alagoas State, Brazil (9°37'52.7" S 35°46'23.1" W)

Site of infection: Base of gill lamellae (basifilamental).

Type-material: A glass with myxospores (hapantotype) was deposited in the collection of the Instituto Nacional de Pesquisa da Amazônia (INPA), Brazil (Num. INPA–CND 000105). The ssrDNA partial sequences were deposited in GenBank with accession number PP926142.

Etymology: The specific name is derived from the host collection site (Mundaú = *mundauensis*)

Description: White plasmodia measuring up to 1 mm at the base of gill lamellae. Mature myxospores elongated in valvular view and oval in sutural views, 5.9–7.1 ( $6.9 \pm 0.6$ )  $\mu\text{m}$  long, 4.9–6.1 ( $5.5 \pm 0.4$ )  $\mu\text{m}$  wide, and 4.2–4.4 ( $4.3 \pm 0.1$ )  $\mu\text{m}$  thick. Mucous envelope, intercapsular appendix absent and edge markings present. Two pyriform polar capsules at the anterior pole of the myxospore, occupying half of the myxospore body, and equal in size, 2.9–3.7 ( $3.2 \pm 0.3$ )  $\mu\text{m}$  long and 1.2–2.0 ( $1.6 \pm 0.2$ )  $\mu\text{m}$  wide. Polar tubules coiled with 4 turns. Sporoplasm single and filled entire space below polar capsules.

### 3.1.2. Taxonomic Summary

Phylum Cnidaria Verrill, 1865

Subphylum Endocnidozoa Schuchert, 1996

Class Myxozoa Grassé, 1970

Subclass Myxosporea Bütschli, 1881

Order Bivalvulida Shulman, 1959

Family Myxobolidae Thélohan, 1892

Genus *Myxobolus* Bütschli, 1882

*Myxobolus patriciae* n. sp. (Figures 3B and 4)



**Figure 4.** Mature myxospores of *Myxobolus patriciae* n. sp. (INPA–CND 000104) found parasitizing the intestine of *Mugil curema*. Highlighted myxospore where it is possible to observe the turns of the polar filament inside the polar capsule.

Type-host: *Mugil curema* Valenciennes, 1836 (Mugiliformes, Mugilidae).

Prevalence: 5 of 42 (11.9%) fish.

Intensity: several plasmodia per parasitized host.

Type-locality: Mundaú lagoon, municipality of Maceió, Alagoas State, Brazil (9°37'52.7" S 35°46'23.1" W)

Site of infection: Intestine (lamina propria).

Type-material: A glass with myxospores (hapantotype) was deposited in the collection of the Instituto Nacional de Pesquisa da Amazônia (INPA), Brazil (Num. INPA–CND 000104). The ssrDNA partial sequences were deposited in GenBank with accession number PP926143.

Etymology: The specific name is derived from a tribute to Patricia Matos who has contributed so much to the study of the biodiversity of Brazilian myxozoans.

Description: White plasmodia measuring on average approximately 0.5 mm in the intestine. Mature myxospores ellipsoidal in valvular and in sutural views, 7.9–9.3 ( $8.6 \pm 0.4$ )  $\mu\text{m}$  long, 8.3–9.3 ( $8.9 \pm 0.3$ )  $\mu\text{m}$  wide, and 4.9–5.8 ( $5.5 \pm 0.2$ )  $\mu\text{m}$  thick. Mucous envelope, intercapsular appendix, and edge markings absent. Two pyriform polar capsules, at the anterior pole of the myxospore, occupying more than half of the myxospore body, and equal in size, 3.8–5.0 ( $4.4 \pm 0.3$ )  $\mu\text{m}$  long and 2.6–3.5 ( $3.0 \pm 0.2$ )  $\mu\text{m}$  wide. Polar tubules coiled with 4–5 turns. Sporoplasm single and filled entire space below polar capsules.

### 3.2. Molecular and Phylogenetic Analysis

One partial ssrDNA sequence of the *M. mundauensis* n. sp. (1800-bp) and one partial ssrDNA sequence of the *Myxobolus patriciae* n. sp. (1523-bp) were obtained. When aligned with each other, the partial sequences of *M. mundauensis* n. sp. and *Myxobolus patriciae* n. sp. showed 89.4% similarity and differed in 165 nucleotides.

The species that most genetically resembles *M. mundauensis* n. sp. was *M. maceioensis* with 91.6% similarity and 145 different nucleotides. The species that most genetically resembles *Myxobolus patriciae* n. sp. was *M. curemae* with 91.4% similarity and 175 different nucleotides including gaps.

Phylogenetic analysis of species genetically similar to the two new species showed a division into three main clades (Figure 5). The main clade is composed of *Myxobolus* spp. that parasitize Mugiliformes. The other two clades are formed by *Henneguya* spp. that parasitize Siluriformes and *Myxobolus* and *Henneguya* spp. that parasitize Characiformes. There is also a clear division into clades by species that parasitize marine and freshwater fish. *Myxobolus maceioensis* appears as a sister species of *M. mundauensis* n. sp., while *M. curemae* appears as a sister species of *Myxobolus patriciae* n. sp.

### 3.3. Remarks

The new species were compared with all *Myxobolus* species already described and showed differences in morphological, morphometric or molecular aspects. When compared to each other, the species showed few similarities, because *Myxobolus patriciae* n. sp. is higher in all measurements observed compared to *M. mundauensis* n. sp. Emphasis was given on comparison with species that parasitize the gills or intestines of Mugiliformes with similar morphometry to the new species (Table 2). The species that most resembled *M. mundauensis* n. sp. was *M. curemae*. There were no observable morphometric differences, but there was a genetic difference of 11.8% (189 different nucleotides) and geographical distance (northeast vs. southeastern Brazil). Furthermore, *M. curemae* has a round myxospore body, while *M. mundauensis* n. sp. presents the body slightly elongated. *Myxobolus bragantinus* Cardim, Silva, Hamoy, Matos & Abrunhosa, 2018 also did not show morphometric differences about *M. mundauensis* n. sp. However, the shape of the body of *M. bragantinus* is spherical, while *M. mundauensis* n. sp. is elongated; there are differences in the host (*Mugil rubrioculus* Harrison, Nirchio, Oliveira, Ron & Gaviria, 2007) and in the region where *M. bragantinus* was described (northern Brazil). Furthermore, when compared molecularly, the partial sequences of the two species showed a difference of 8% in nucleotides. The partial sequence of *M. bragantinus* was not used in the phylogenetic analysis due to its

small size (992 bp). Regarding species that parasitize other families of hosts or other organs, the species that most resembled *M. mundauensis* n. sp. was *Myxobolus nigeriae* Dar, Kaur & Chisti, 2016. There are no major morphometric differences between the species, but morphologically *M. nigeriae* appears ovoid or subspherical, while *M. mundauensis* n. sp. is elongated. Furthermore, *M. nigeriae* was described as parasitizing the gills of *Schizopyge niger* (Heckel, 1838) from India, having a host and geographical location far from the new species. Unfortunately, there is no *M. nigeriae* genetic sequence available for comparison. *Myxobolus imparfinis* Vieira, Tagliavini, Abdallah & Azevedo, 2018 also has morphometry similar to the new species. However, it was described as parasitizing the gills of *Imparfinis mirini* Haseman, 1911, a freshwater fish from Brazil. Furthermore, there is a difference in the length of the myxospore, as the range in *M. mundauensis* n. sp. was 5.9–7.1 while in *M. imparfinis* it was 7.1–8.4.

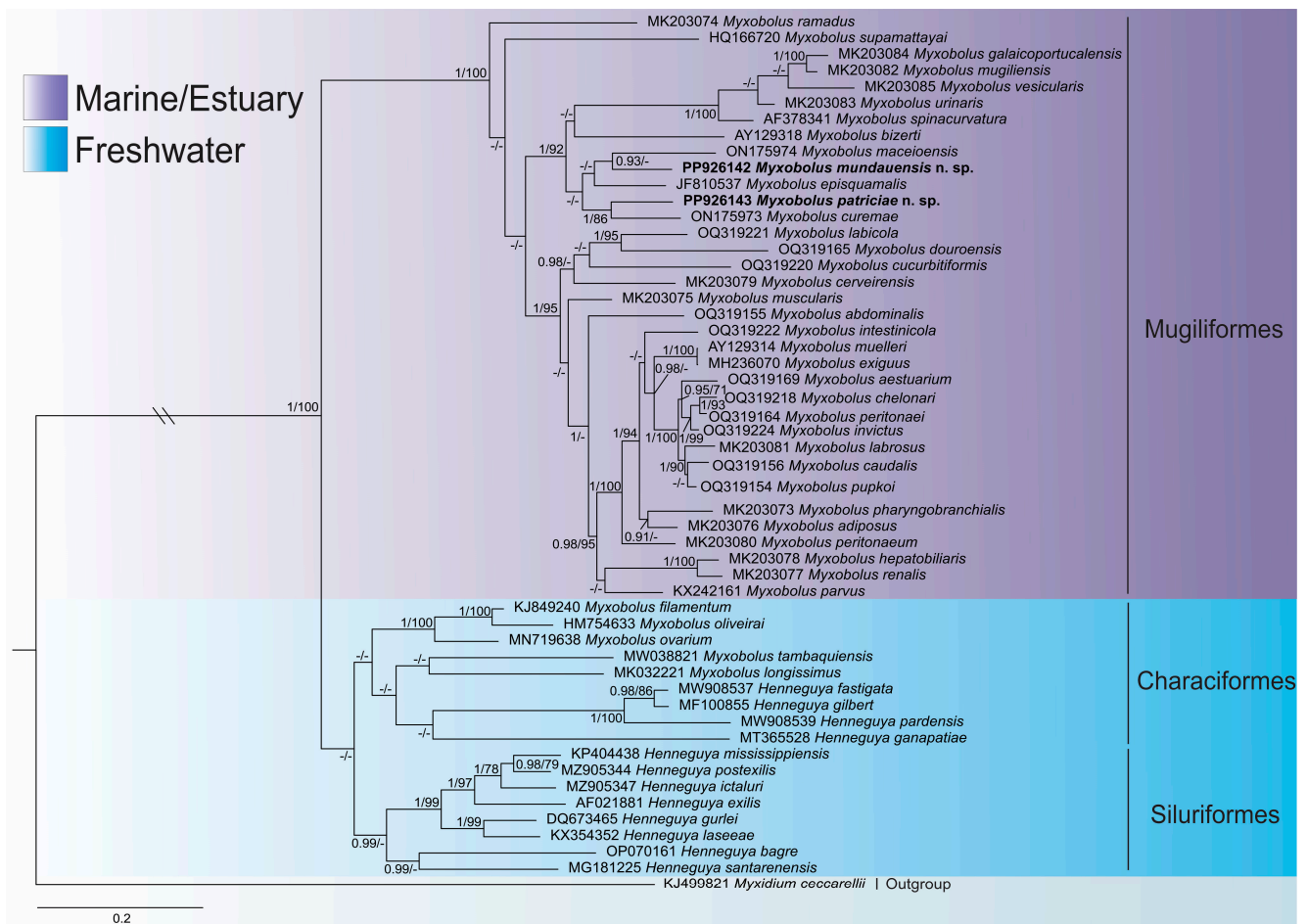


**Figure 5.** Phylogenetic tree of Bayesian inference analysis based on partial ssrDNA sequences showing the position of *Myxobolus mundauensis* n. sp. and *Myxobolus patriciae* n. sp. among other genetically similar *Henneguya*/*Myxobolus* species. Node numbers represent respectively posterior probabilities for Bayesian inference (BI) and bootstraps for the maximum-likelihood (ML). Values less than 0.9 for BI and 70 for ML are represented by dashes. The scale bar represents the number of substitutions per site.

**Table 2.** Morphometric comparison for *Myxobolus mundauensis* n. sp. and *Myxobolus patriciae* n. sp. (in bold) with *Myxobolus* spp. that parasitize the gills and intestine of mullets with similar morphometry to the new species. SBP: spore body length; SPW: spore body width; LP: length of polar capsules; WP: width of polar capsules; T: thickness; TP: number of turns of polar filaments. The measurements are given in  $\mu\text{m}$ . The standard deviation is given after the values.

Species	SBL	SPW	T	LP	WP	TP	Host	Site of Infection	Country	Reference
<i>M. mundauensis</i> n. sp.	<b>6.9 ± 0.3</b> (5.9–7.1)	<b>5.5 ± 0.4</b> (4.9–6.1)	<b>4.3 ± 0.1</b> (4.2–4.4)	<b>3.2 ± 0.2</b> (2.9–3.7)	<b>1.6 ± 0.2</b> (1.2–2.0)	4	<i>Mugil curema</i>	Gills	Brazil	Present study
<i>M. aestuarium</i>	7.8 ± 0.3	7.1 ± 0.7	5.1 ± 0.3	3.4 ± 0.2	2.1 ± 0.2	3–4	<i>Chelon labrosus</i>	Gills	Portugal	[14]
<i>M. bragantinus</i>	6.2 ± 0.3	6.2 ± 0.3	-	2.4 ± 0.3	1.5 ± 0.2	-	<i>Mugil rubriolocus</i>	Gills	Brazil	[37]
<i>M. chelonari</i>	8.3 ± 0.2	7.1 ± 0.4	-	3.9 ± 0.2	2.3 ± 0.1	3–4	<i>Chelon labrosus</i>	Gills	Portugal	[14]
<i>M. curemae</i>	6.5 ± 0.3	5.9 ± 0.4	5.0 ± 0.3	3.0 ± 0.3	1.9 ± 0.2	4	<i>Mugil curema</i>	Gills	Brazil	[38]
<i>M. douroensis</i>	8.2 ± 0.3	7.3 ± 0.2	5.6 ± 0.2	3.9 ± 0.2	2.5 ± 0.2	3–4	<i>Chelon labrosus</i>	Gills	Portugal	[14]
<i>M. hani</i>	8.0 ± 0.4	7.1 ± 0.3	-	-	-	-	<i>Mugil curema</i>	Gills	Senegal	[21]
<i>M. invictus</i>	8.5 ± 0.2	7.9 ± 0.2	-	3.6 ± 0.2	2.0 ± 0.1	3	<i>Chelon labrosus</i>	Gills	Portugal	[14]
<i>M. maceioensis</i>	7.2 ± 0.5	7.1 ± 0.6	5.0 ± 0.2	3.6 ± 0.3	2.2 ± 0.2	4	<i>Mugil curema</i>	Gills	Brazil	[38]
<i>M. parous</i>	6.5–7	5.5–6	4–4.2	3.8–4.2	2.0	-	<i>Liza saliens</i>	Gills	Turkey	[39]
<i>M. pupkoi</i>	8.4 ± 0.3	7.7 ± 0.4	5.1 ± 0.3	3.2 ± 0.2	2.0 ± 0.2	3–4	<i>Chelon labrosus</i>	Gills	Portugal	[14]
<i>M. ramadus</i>	8.2 ± 0.5	7.9 ± 0.2	6.4 ± 0.2	4.2 ± 0.2	3.0 ± 0.3	5–6	<i>Chelon ramada</i>	Gills	Portugal	[40]
<i>M. saladensis</i>	10.0 ± 11.1	9.2 ± 0.5	-	3.8 ± 0.2	2.3 ± 0.1	4–5	<i>Mugil liza</i>	Gills	Argentina	[41]
<i>M. patriciae</i> n. sp.	<b>8.6 ± 0.4</b> (7.9–9.3)	<b>8.9 ± 0.3</b> (8.3–9.3)	<b>5.5 ± 0.2</b> (4.9–5.8)	<b>4.4 ± 0.3</b> (3.8–5.0)	<b>3.0 ± 0.2</b> (2.6–3.5)	5–6	<i>Mugil curema</i>	Intestine	Brazil	Present study
<i>M. intestinicola</i>	7.7 ± 0.3	6.5 ± 0.3	5.6 ± 0.2	3.4 ± 0.3	2.1 ± 0.2	4–5	<i>Chelon labrosus</i>	Intestine	Portugal	[14]
<i>M. cerveirensis</i>	8.1 ± 0.2	6.8 ± 0.2	5.3 ± 0.3	4.2 ± 0.2	2.8 ± 0.2	4–5	<i>Chelon ramada</i>	Intestine	Portugal	[40]
<i>M. lizae</i>	9.0–9.5	4.6–5.2	-	3.2	2.0	5–7	<i>Planiliza</i>	Intestine	India	[42]
<i>M. adeli</i>	6.2 ± 0.3	7.2 ± 0.3	4.6 ± 0.4	3.1 ± 0.3	1.8 ± 0.2	4	<i>Macrolepis</i> <i>Liza aurata</i>	Intestine	Japan	[43]

Regarding the species that parasitize intestines from Mugiliformes, the species that most closely resembles *Myxobolus patriciae* n. sp. was *M. cerveirensis*. Although there are similarities between species, the main difference is in the width of the myxospore body ( $8.9 \pm 0.3$  vs.  $6.8 \pm 0.2$ ). Regarding the molecular comparison, there was a difference of 13% in nucleotides concerning the available partial sequences of both species. In addition, *M. cerveirensis* was described in the intestine of *Chelon ramada* (Risso, 1827) from Portugal, with differences in host and geographic region. *Myxobolus intestinicola* has a smaller body in width than *M. patriciae* n. sp. ( $8.9 \pm 0.3$  vs.  $6.5 \pm 0.3$ ) and their polar capsules are smaller ( $4.4 \pm 0.3$  vs.  $3.4 \pm 0.3$ ), while *M. adeli* has a smaller body in length ( $8.6 \pm 0.4$  vs.  $6.2 \pm 0.3$ ). Regarding species that parasitize other families of hosts or other organs, the species that most resembled *M. patriciae* n. sp. is *Myxobolus adiposus* Rocha, Casal, Alves, Antunes, Rodrigues & Azevedo 2019 that parasitizes the adipose tissue of *Chelon ramada* (Risso, 1827). There are no major morphometric or morphological differences between the species; however, our phylogenetic analysis shows a great molecular difference between species that have different hosts. *Myxobolus xinyangensis* Wu, Wang, Sato & Zhang, 2019, which parasitizes the muscles of *Abbottina rivularis* (Basilewsky, 1855), also presents similar morphometry to *M. patriciae* n. sp. However, *M. xinyangensis* has larger polar capsules ( $5.6 \pm 0.67$  vs.  $4.4 \pm 0.3$ ) and bigger thickness ( $6.4 \pm 0.28$  vs.  $5.5 \pm 0.2$ ) than those found in *M. patriciae* n. sp., differentiating the two species.

#### 4. Discussion

We present two new *Myxobolus* species, *M. mundauensis* n. sp. found in the gills and *M. patriciae* n. sp. found in the intestine, characterized by morphology, host specificity, tissue tropism, and molecular features. The BI phylogenetic analysis conducted in this study

distinctly separates these novel species from other *Myxobolus* species with sequences accessible in the NCBI database. Their closest evolutionary relationship with species parasitizing Mugiliformes underscores the significant influence of host order on the phylogenetic positioning of myxosporeans, corroborating recent research findings [20,25]. This investigation provides further evidence supporting the coevolutionary dynamics between myxosporeans and their vertebrate hosts, with all authentic mugiliform-infecting myxobolids forming a well-supported monophyletic subclade.

Histoziotic myxozoan species are considered to be the most pathogenic [44], with some being potentially fatal [45]. *Myxobolus* species can induce lesions that serve as entry points for secondary viral and bacterial infections upon cyst rupture, releasing mature spores [46]. Only a select few myxozoan species exhibit a preference for parasitizing the intestine [44]. Among the most extensively studied myxozoans infecting the gastrointestinal tract are *Enteromyxum* spp. and *Ceratomyxa shasta*, both capable of inflicting severe damage to the intestinal epithelium and causing chronic enteritis [47–52]. *Myxobolus nodulointestinalis* Masmoumian, Baska & Molnár, 2006 was described parasitizing the intestine of *Mesopotamichthys sharpeyi* (Günther, 1874) and caused a deep bulge in the intestinal lumen and intestinal cavity, leading to tissue deformations and a small degeneration of the muscle layer [53]. In this study, no clinical symptoms were observed for the mullets and no obvious pathology due to *Myxobolus mundauensis* n. sp. and *Myxobolus patriciae* n. sp. was appreciable. Regarding the gills, plasmodia on different sites can inflict different degrees of damage to the health of the host [54]. For example, *Myxobolus basilamellaris* Lom & Molnár, 1983 develops between the afferent and efferent arterial vessels of the base of gill filaments and causes ischemic necrosis of the gill, which can cause fish death due to gill failure [55]. However, in heavily infected gills and intestines, quite large areas of the organ were replaced by plasmodia, with a possible interference in normal physiology. More studies need to be carried out to confirm the degree of pathogenicity of the new species to the hosts.

In the present study, novel species of myxozoans were characterized based on morphology, bolstered by phylogenetic investigation. The combined evidence definitively confirmed the presence of two new species, designated as *M. mundauensis* n. sp. and *M. patriciae* n. sp. Based on our findings, we advocate continual monitoring of these parasites in aquaculture settings to evaluate potential pathogenic impacts that they may elicit. The current study significantly enhances our understanding of the myxosporean diversity infecting *Mugil curemae*, showcasing the breadth of myxosporean fauna that can infect a single host species.

**Author Contributions:** D.H.M.D.V.: Formal analysis, Data curation and Writing—original draft. M.M.O.-P.: Phylogeny analysis and editing. V.D.A.: Supervision, Writing—review and editing and Project Administration. S.L.P.O.: Investigation and Methodology. A.G.T.D.: Investigation and Methodology. R.J.d.S.: Funding acquisition and Resources. R.K.d.A.: Supervision, Writing—review and editing and Project Administration. All authors have read and agreed to the published version of the manuscript.

**Funding:** This work was supported by Fundação de Amparo à Pesquisa do Estado de São Paulo (FAPESP) [grant numbers 2020/05412-9 and 2019/25223-9], Fundação de Amparo à Pesquisa do Estado de Alagoas (FAPEAL) [grant number 60030.0000000464/2020] and Conselho Nacional de Desenvolvimento Científico e Tecnológico–CNPq [grant number 309125/2017-0].

**Data Availability Statement:** The raw data supporting the conclusions of this article will be made available by the authors on request.

**Conflicts of Interest:** The authors declare that they have no known competing financial interests or personal relationships that could have appeared to influence the work reported in this paper.

## References

1. Crosetti, D.; Blaber, S.J. *Biology, Ecology and Culture of Grey Mulletts (Mugilidae)*, 1st ed.; CRC Press: Boca Raton, FL, USA, 2016.
2. Froese, R.; Pauly, D. FishBase. Available online: <https://www.fishbase.org/> (accessed on 4 September 2023).

3. Marin, E.B.J.; Quintero, A.; Bussière, D.; Dodson, J.J. Reproduction and recruitment of white mullet (*Mugil curema*) to a tropical lagoon (Margarita Island, Venezuela) as revealed by otolith microstructure. *Fish Bull.* **2003**, *101*, 809–821.
4. Trape, S.; Durand, J.D.; Vigliola, L.; Panfili, J. Recruitment success and growth variability of mugilids in a West African estuary impacted by climate change. *Estuar. Coast. Shelf Sci.* **2017**, *198*, 53–62. [[CrossRef](#)]
5. Mai, A.C.G.; Santos, M.L.D.; Lemos, V.M.; Vieira, J.P. Discrimination of habitat use between two sympatric species of mullets, *Mugil curema* and *Mugil liza* (Mugiliformes: Mugilidae) in the rio Tramandaí Estuary, determined by otolith chemistry. *Neotrop. Ichtyol.* **2018**, *16*, 1–8. [[CrossRef](#)]
6. Avigliano, E.; Ibañez, A.; Fabré, N.; Fortunato, R.C.; Méndez, A.; Pisonero, J.; Volpedo, A.V. White mullet *Mugil curema* population structure from Mexico and Brazil revealed by otolith chemistry. *J. Fish Biol.* **2020**, *97*, 1187–1200. [[CrossRef](#)] [[PubMed](#)]
7. Ibañez, A.L.; Colín, A. Reproductive biology of *Mugil curema* and *Mugil cephalus* from western Gulf of Mexico waters. *Bull. Marine Sci.* **2014**, *90*, 941–952. [[CrossRef](#)]
8. Cicero, L.H.; Souza, U.P.; Rotundo, M.M.; Pereira, C.D.S.; Sadauskas-Henrique, H. Biometric and hematological indices of *Mugil curema* inhabiting two Neotropical estuaries. *Reg. Stud. Mar. Sci.* **2020**, *38*, 101377. [[CrossRef](#)]
9. Albieri, R.J.; Araújo, F.G.; Uehara, W. Differences in reproductive strategies between two co-occurring mullets *Mugil curema* Valenciennes 1836 and *Mugil liza* Valenciennes 1836 (Mugilidae) in a tropical bay. *Trop. Zool.* **2010**, *23*, 51–62.
10. Lima, A.R.B.; Torres, R.A.; Jacobina, U.P.; Pinheiro, M.A.A.; Adam, M.L. Genomic damage in *Mugil curema* (Actinopterygii: Mugilidae) reveals the effects of intense urbanization on estuaries in northeastern Brazil. *Marin. Pollut. Bull.* **2019**, *138*, 63–69. [[CrossRef](#)] [[PubMed](#)]
11. Okamura, B.; Gruhl, A.; Bartholomew, J.L. *Myxozoan Evolution, Ecology and Development*, 1st ed.; Springer: Berlin/Heidelberg, Germany, 2015.
12. Eiras, J.C.; Molnár, K.; Lu, Y.S. Synopsis of the species of *Myxobolus* Bütschli, 1882 (Myxozoa: Myxosporae: Myxobolidae). *Syst. Parasitol.* **2005**, *61*, 1–46. [[CrossRef](#)]
13. Eiras, J.C.; Cruz, C.F.; Saraiva, A.; Adriano, E.A. Synopsis of the species of *Myxobolus* (Cnidaria, Myxozoa, Myxosporae) described between 2014 and 2020. *Folia Parasitol.* **2021**, *68*, 12. [[CrossRef](#)]
14. Guimarães, J.; Casal, G.; Alves, Â.; Araújo, C.; Rocha, S. Myxozoan survey of thicklip grey mullet *Chelon labrosus* reinforces successful radiation of *Myxobolus* in mugiliform hosts. *Parasite* **2023**, *30*, 26. [[CrossRef](#)] [[PubMed](#)]
15. Maeno, Y.; Sorimachi, M.; Ogawa, K.; Egusa, S. *Myxobolus spinacurvatura* sp. n. (Myxosporae, Bilvalvulida) parasitic in deformed mullet, *Mugil cephalus*. *Fish Pathol.* **1990**, *25*, 37–41. [[CrossRef](#)]
16. Bahri, S.; Marques, A. Myxosporae parasites of the genus *Myxobolus* from *Mugil cephalus* in Ichkeul lagoon, Tunisia: Description of two new species. *Dis. Aquat. Org.* **1996**, *27*, 115–122. [[CrossRef](#)]
17. Eiras, J.C.; D'Souza, J. *Myxobolus goensis* n. sp. (Myxozoa, Myxosporae, Myxobolidae), a parasite of the gills of *Mugil cephalus* (Osteichthyes, Mugilidae) from Goa, India. *Parasite* **2004**, *11*, 243–248. [[CrossRef](#)]
18. Eiras, J.C.; Abreu, P.C.; Robaldo, R.; Junior, J.P. *Myxobolus platanus* n. sp. (Myxosporae, Myxobolidae), a parasite of *Mugil platanus* Gunther, 1880 (Osteichthyes, Mugilidae) from Lagoa dos Patos, RS, Brazil. *Arq. Bras. Med. Vet. Zootec.* **2007**, *59*, 895–898. [[CrossRef](#)]
19. Kim, W.S.; Kim, J.H.; Oh, M.J. Morphologic and Genetic Evidence for Mixed Infection with Two *Myxobolus* Species (Myxozoa: Myxobolidae) in Gray Mullet, *Mugil cephalus*, from Korean Waters. *Korean J. Parasitol.* **2013**, *51*, 369–373. [[CrossRef](#)]
20. Rocha, S.; Azevedo, C.; Oliveira, E.; Alves, A.; Antunes, C.; Rodrigues, P.; Casal, G. Phylogeny and comprehensive revision of mugiliform-infecting myxobolids (Myxozoa, Myxobolidae), with the morphological and molecular redescription of the cryptic species *Myxobolus exiguus*. *Parasitology* **2019**, *146*, 479–496. [[CrossRef](#)] [[PubMed](#)]
21. Faye, N.; Kpatcha, T.K.; Debakate, C.; Fall, M.; Toguebaye, B.S. Gill infections due to myxosporae (myxozoa) parasites in fishes from Senegal with description of *Myxobolus hani* sp. n. *Bull. Eur. Assoc. Fish Pathol.* **1999**, *19*, 14–16.
22. Faye, N.; Kpatcha, T.K.; Fall, M.; Toguebaye, B.S. Heart infections due to myxosporae (Myxozoa) parasites in marine and estuarine fishes from Senegal. *Bull. Eur. Assoc. Fish Pathol.* **1997**, *17*, 115–117.
23. Lom, J.; Arthur, J.R. A guideline for the preparation of species descriptions in Myxosporae. *J. Fish Dis.* **1989**, *12*, 151–156. [[CrossRef](#)]
24. Bush, A.O.; Lafferty, K.D.; Lotz, J.M.; Shostak, A.W. Parasitology meets ecology on its own terms: Margolis et al. revisited. *J. Parasitol.* **1997**, *83*, 575–583. [[CrossRef](#)] [[PubMed](#)]
25. Vieira, D.H.M.D.; Narciso, R.B.; da Silva, R.J. Morphological and molecular characterization of the cryptic species *Myxobolus cataractae* n. sp. (Cnidaria: Myxozoa: Myxobolidae) parasitizing *Imparfinis mirini* (Siluriformes: Heptapteridae). *Parasitol. Int.* **2022**, *88*, 102560. [[CrossRef](#)] [[PubMed](#)]
26. Barta, J.R.; Martin, S.D.; Liberator, P.A.; Dashkevich, M.; Anderson, J.W.; Feighner, S.D.; Elbrecht, A.; Perkins-Barrow, A.; Jenkins, M.C.; Danforth, H.D. Phylogenetic relationships among eight *Eimeria* species infecting domestic fowl inferred using complete small subunit ribosomal DNA sequences. *J. Parasitol.* **1997**, *83*, 262–271. [[CrossRef](#)] [[PubMed](#)]
27. Kent, M.L.; Khattra, J.; Hedrick, R.P.; Devlin, R.H. *Tetracapsula renicola* n. sp. (Myxozoa: Saccosporidae); The PKX myxozoan—The cause of proliferative kidney disease of salmonid fishes. *J. Parasitol.* **2000**, *86*, 103–111. [[CrossRef](#)] [[PubMed](#)]
28. Hallett, S.L.; Diamant, A. Ultrastructure and small-subunit ribosomal DNA sequence of *Henneguya lesteri* n. sp. (Myxosporae), a parasite of sand whiting *Sillago analis* (Sillaginidae) from the coast of Queensland, Australia. *Dis. Aquat. Org.* **2001**, *46*, 197–212. [[CrossRef](#)] [[PubMed](#)]

29. Eszterbauer, E. Genetic relationship among gill-infecting *Myxobolus* species (Myxosporea) of cyprinids: Molecular evidence of importance of tissue-specificity. *Dis. Aquat. Org.* **2004**, *58*, 35–40. [[CrossRef](#)] [[PubMed](#)]
30. Andree, K.B.; Szekely, C.; Molnár, K.; Gresoviac, S.J.; Hedrick, R.P. Relationships among members of the genus *Myxobolus* (Myxozoa: Bilvalvidae) based on small subunit ribosomal DNA sequences. *J. Parasitol.* **1999**, *85*, 68–74. [[CrossRef](#)] [[PubMed](#)]
31. Kearse, M.; Moir, R.; Wilson, A.; Stones-Havas, S.; Cheung, M.; Sturrock, S.; Buxton, S.; Cooper, A.; Markowitz, S.; Duran, C. Geneious Basic: An integrated and extendable desktop software platform for the organization and analysis of sequence data. *Bioinformatics* **2012**, *28*, 1647–1649. [[CrossRef](#)] [[PubMed](#)]
32. Larkin, M.A.; Blackshields, G.; Brown, N.P.; Chenna, R.; Mcgettigan, P.A.; McWilliam, H.; Valentin, F.; Wallace, I.M.; Wilm, A.; Lopez, R.; et al. Clustal W and Clustal X version 2.0. *Bioinformatics* **2007**, *23*, 2947–2948. [[CrossRef](#)]
33. Ronquist, F.; Huelsenbeck, J.P. MrBayes 3: Bayesian phylogenetic inference under mixed models. *Bioinformatics* **2003**, *19*, 1572–1574. [[CrossRef](#)]
34. Guindon, S.; Gascuel, O. A simple, fast, and accurate algorithm to estimate large phylogenies by maximum likelihood. *Syst. Biol.* **2003**, *52*, 696–704. [[CrossRef](#)]
35. Miller, M.A.; Pfeiffer, W.; Schwartz, T. Creating the CIPRES Science Gateway for inference of large phylogenetic trees. In Proceedings of the 2010 Gateway Computing Environments Workshop (GCE), New Orleans, LA, USA, 14 November 2010; pp. 1–8. [[CrossRef](#)]
36. Rambaut, A. *FigTree 1.4.2. Software*; Institute of Evolutionary Biology, University Edinburgh: Edinburgh, UK, 2014.
37. Cardim, J.; Silva, D.; Hamoy, I.; Matos, E.; Abrunhosa, F. *Myxobolus bragantinus* n. sp. (Cnidaria: Myxosporea) from the gill filaments of the redeye mullet, *Mugil rubrioculus* (Mugiliformes: Mugilidae), on the eastern Amazon coast. *Zootaxa* **2018**, *4482*, 177–187. [[CrossRef](#)]
38. Vieira, D.H.M.D.; Agostinho, B.N.; Negrelli, D.C.; Silva, R.J.; Azevedo, R.K.; Abdallah, V.D. Taxonomy and Systematics of Two New Species of *Myxobolus* (Cnidaria: Myxobolidae) Parasitizing the Gills of *Mugil curema* (Mugilidae) from the Brazilian Coast. *Acta Parasitol.* **2022**, *67*, 1206–1216. [[CrossRef](#)]
39. Shulman, S.S.; Protozoa, P. *Bykhovskaya-Pavlovskaya, I.E. Key to Parasites of Freshwater Fishes of the USSR*; Keys to Fauna of the USSR, No. 80; Nauka: Leningrad, Russia, 1962; pp. 7–151.
40. Rocha, S.; Casal, G.; Alves, Â.; Antunes, C.; Rodrigues, P.; Azevedo, C. Myxozoan biodiversity in mullets (Teleostei, Mugilidae) unravels hyperdiversification of *Myxobolus* (Cnidaria, Myxosporea). *Parasitol. Res.* **2019**, *118*, 3279–3305. [[CrossRef](#)]
41. Marcotegui, P.; Martorelli, S. *Myxobolus saladensis* sp. nov., a new species of gill parasite of *Mugil liza* (Osteichthyes, Mugilidae) from Samborombón Bay, Buenos Aires, Argentina, Iheringia. *Sér. Zool.* **2017**, *107*, e2017026. [[CrossRef](#)]
42. Narasimhamurti, C.C.; Kalavati, C. *Myxosoma lairdi* n. sp. (Protozoa: Myxosporidia) parasitic in the gut of the estuarine fish, *Liza macrolepis* Smith. *Proc. Anim. Sci.* **1979**, *88*, 269–272.
43. Yurakhno, V.M.; Ovcharenko, M.O. Study of Myxosporea (Myxozoa), infecting worldwide mullets with description of a new species. *Parasitol. Res.* **2014**, *113*, 3661–3674. [[CrossRef](#)]
44. Gomez, D.; Bartholomew, J.L.; Sunyer, J.O. Biology and mucosal immunity to myxozoans. *Develop. Comp. Immunol.* **2014**, *43*, 243–256. [[CrossRef](#)]
45. Lom, J.; Dyková, I. Myxozoan genera: Definition and notes on taxonomy, life-cycle terminology and pathogenic species. *Folia Parasitol.* **2006**, *53*, 1–36. [[CrossRef](#)]
46. Feist, S.W.; Longshaw, M. Phylum Myxozoa. In *Fish Diseases and Disorders*; Woo, P.T.K., Ed.; Volume 1: Protozoan and Metazoan Infections; CABI: Wallingford, UK, 2006; pp. 230–296. [[CrossRef](#)]
47. Bartholomew, J.L. Host resistance to infection by the myxosporean parasite *Ceratomyxa shasta*: A review. *J. Aquat. Anim. Health* **1998**, *10*, 112–120. [[CrossRef](#)]
48. Bartholomew, J.L.; McDowell, T.S.; Hedrick, R.P. Susceptibility of rainbow trout resistant to *Myxobolus cerebralis* to selected salmonid pathogens. In *Propagated Fish in Resource Management*; Nickum, M.J., Mazik, P.M., Nickum, J.G., Mackinlay, D.D., Eds.; American Fisheries Society: New York, NY, USA, 2004; pp. 549–557.
49. Sitjá-Bobadilla, A.; Palenzuela, O.; Riaza, A.; Macias, M.A.; Alvarez-Pellitero, P. Protective acquired immunity to *Enteromyxum scophthalmi* (myxozoa) is related to specific antibodies in *Psetta maxima* (L.) (Teleostei). *Scand. J. Immunol.* **2007**, *66*, 26–34. [[CrossRef](#)]
50. Fleurance, R.; Sauvegrain, C.; Marques, A.; Le Breton, A.; Guereaud, C.; Cherel, Y.; Wyers, M. Histopathological changes caused by *Enteromyxum leei* infection in farmed sea bream *Sparus aurata*. *Dis. Aquat. Org.* **2008**, *79*, 219–228. [[CrossRef](#)]
51. Alvarez-Pellitero, P.; Palenzuela, O.; Sitjá-Bobadilla, A. Histopathology and cellular response in *Enteromyxum leei* (Myxozoa) infections of *Diplodus puntazzo* (Teleostei). *Parasitol. Int.* **2008**, *57*, 110–120. [[CrossRef](#)]
52. Bjork, S.J.; Bartholomew, J.L. Invasion of *Ceratomyxa shasta* (Myxozoa) and comparison of migration to the intestine between susceptible and resistant fish hosts. *Int. J. Parasitol.* **2010**, *40*, 1087–1095. [[CrossRef](#)]
53. Masoumian, M.; Baska, F.; Molnár, K. *Myxobolus nodulointestinalis* sp. n. (Myxosporea; Myxobolidae), a parasite of the intestine of *Barbus sharpeyi*. *Dis. Aquat. Org.* **1996**, *24*, 35–39. [[CrossRef](#)]

- 
54. Zhang, J.; Wang, Y.; Zhao, Y. The description of *Myxobolus meijiangensis* n. sp. (Myxozoa: Myxobolidae) and its pathogenicity to the gills of goldfish. *Parasitol. Int.* **2023**, *97*, 102795. [[CrossRef](#)]
  55. Wang, M.M.; Zhang, J.Y.; Zhao, Y.J. New record for *Myxobolus basilemellaris* in China with histopathological insights into gill infestation. *J. Fish. China* **2021**, *45*, 1555–1562. [[CrossRef](#)]

**Disclaimer/Publisher’s Note:** The statements, opinions and data contained in all publications are solely those of the individual author(s) and contributor(s) and not of MDPI and/or the editor(s). MDPI and/or the editor(s) disclaim responsibility for any injury to people or property resulting from any ideas, methods, instructions or products referred to in the content.